Investigation of Acetyl Ferrocene Migration from Hydroxyl-Terminated Polybutadiene Based Elastomers by Means of Ultraviolet–Visible and Atomic Absorption Spectroscopic Techniques

Alper Ünver,[1] Nursel Dilsiz,[2] Mürvet Volkan,[1] Güneri Akovalı[1]

[1]*Department of Chemistry, Middle East Technical University, 06531 Ankara, Turkey*
[2]*Department of Chemical Engineering, Gazi University, 06570 Ankara, Turkey*

Received 12 January 2004; accepted 18 October 2004
DOI 10.1002/app.21624

ABSTRACT: Migration and leakage of some mobile components in rocket propellant produces an inhomogeneous composition region at which migration takes place, which can lead to premature detonation, changes in ballistic characteristics, and so on. It is, therefore, important to be able to predict the behavior of low-molecular-weight mobile additives and to control the leakage of them from the propellant. At this point, our chief interest was to study the magnitude of the migration and to understand the factors that influence the migration process. In this study, the migration of a ferrocene-based burning-rate catalyst [acetyl ferrocene (AcF)] a from hydroxyl-terminated polybutadiene (HTPB) based elastomer in the presence of a plasticizer (dioctyl adipate) was examined in accelerated aging conditions at 60°C for various time intervals. We also tried to minimize the migration of AcF from the loaded to the unloaded part by using an extra barrier layer consisting of polyfunctional aziridine (AST D45+) in addition to the HTPB–toluene diisocyanate composition. The migration enhanced with aging of the AcF and the barrier effects of the layer with intensified crosslink density to this migration were studied extensively. The migration was monitored by both ultraviolet–visible and atomic absorption spectroscopy (AAS) methods. A comparison of the data obtained from both of these methods was also done. The two techniques were found to be in agreement, and the Fe determinations from both methods were highly correlated, suggesting that the data were reliable, although the AAS data were found to be symmetrically somewhat higher. © 2005 Wiley Periodicals, Inc. J Appl Polym Sci 96: 1654–1661, 2005

Key words: HTPB; burn-rate catalyst; aging; migration; UV–vis

INTRODUCTION

Solid rocket propellants can be regarded as highly filled polymers. The propellant generally consists of about 85 wt % explosive particulate embedded in about 15 wt % elastomeric binder. So, in these highly filled network systems, the migration of some mobile components from more highly concentrated regions to lower ones is not a surprising situation. In migrational motion, individual molecules of the liquid move by "jumping" into adjacent holes formed in the elastomeric matrix during random thermal motions, which arise from kinetic energy. The thermodynamic drive is due to a tendency to equalize the chemical potential (i.e., concentration) of the diffusing liquid throughout the elastomer. There is no real force pushing molecules down the slope of chemical potential, for that is their natural drift as a consequence of the second law and the hunt for maximum entropy.

Migration occurs in elastomeric systems as a result of concentration differences in mobile species across bimaterial interfaces (Fig. 1). If the mobile species are not chemically bonded to a substrate material, they will migrate in the direction of lower concentrations. Fick's law governs simple migration and is given in eq. (1):

$$\left(\frac{\partial c}{\partial t}\right) = D\left(\frac{\partial^2 c}{\partial x^2}\right) \tag{1}$$

where c is the concentration, t is the time, x is the distance, and the parameter D is the diffusivity, which is a measure of the mobility of the migrating species.

The migration of low-molecular-weight additives, such as plasticizers and burn-rate catalysts, from the propellant into the insulation during curing and aging processes can be extremely hazardous.

Many studies have been done to date on the accelerated aging of laboratory-scale-produced propellant samples. In these studies, it has been reported that the aging rate is strongly dependent on the used storage conditions.[1–3] Moreover, some predictions have been

---

Correspondence to: A. Ünver (aunver@metu.edu.tr).

Journal of Applied Polymer Science, Vol. 96, 1654–1661 (2005)

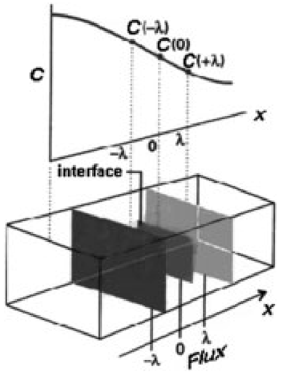

Figure 1 Migration profile of a migrating specimen.

made about the long-time mechanical property behaviors and burn-rate characteristics of the propellant systems.[4–6] There are some studies in literature about the acceleration of migration in propellant systems by aging.[7–9] These studies have confirmed the existence of burn-rate catalyst migration in the propellant adjacent to the insulation during aging. With the overaging of porous grain, a significant chemical change in the propellant composition occurs, especially in insulation regions due to migration or slow, low-order chemical reactions. This can reduce the allowable physical properties, weakening the grain, so that it will crack at stress-concentrated points and cause unfavorable increases or fluctuations in the burning rate and performance of the rocket motor.[10]

The aging of a propellant can be measured with sample tests if the loading during the life of the motor can be correctly anticipated. It is then possible to estimate and predict the useful shelf life, or storage life, of a rocket motor. The life of a particular motor depends on the particular propellant, the frequency and the magnitude of imposed loads or strains, the design, and other factors. Typical life values range from 5 to 25 years. Shelf life can usually be increased by increasing the physical strength of the propellants (e.g., by increasing the amount of binder); selecting chemically compatible, stable ingredients with minimal long-term degradation; reducing migration to a minimum from propellant grain to insulation; and by minimizing the vibration loads, temperature limits, and number of cycles (controlled storage and transport environment).[10]

Virtually every burning-rate accelerator is made of mineral or organic metallic byproducts of copper, iron, chromium, or boron.[11] Simple ferrocene compounds are commonly used as burn-rate catalysts in composite solid propellants, mainly because of the better ignitability of the propellant compared to ones containing conventional inert solid catalysts such as ferric oxide (Fe_2O_3) and copper chromite (CuCr). In addition, ferrocene catalysts can be loaded up to 9 wt % of the propellant to achieve very high burn rates with the rheological and mechanical properties of the propellant remaining within an acceptable limit. On the other hand, the loading of conventional catalysts beyond 2 wt % significantly damages the mechanical properties of the propellant and its processing characteristics because of commonly encountered agglomeration. However, the use of ferrocene derivatives as burn-rate catalyst brings about some setbacks, such as their migration to insulation during curing and storage, evaporation or sublimation loss during processing, and phase separation by crystallization in low-temperature applications or storage. To preclude these problems and also to enhance the efficiency of ferrocene-based burn-rate catalysts, several attempts have been made with appropriate ferrocene derivatives to covalently link the ferrocene moiety to the preformed propellant binder via grafting, to the binder backbone during its synthesis, and to the network during its formation in the propellant processing.[12,13]

In this study, the migration of acetyl ferrocene (AcF), which was used as the burn-rate catalyst, in the accelerated aging of a hydroxyl-terminated polybutadiene (HTPB) based elastomeric system was studied. The migrated amount of the AcF in the nonloaded part at different distances from the loaded part was determined with ultraviolet–visible (UV–vis) spectroscopy and atomic absorption spectroscopy (AAS) after a definite aging period and was compared with the initial AcF concentration. In addition to the effect of the aging period on the degree of migration, the barrier effect of a specially prepared layer was examined. The migration was studied by measurement of the mass concentration of AcF in the HTPB samples at various distances from the insulation at definite intervals of aging. Studies were conducted to examine the effect of aging time on the migration process.

AAS is used extensively in the determination of metal ions. The critical steps in the analysis are the dissolution of the samples and the elimination of the interferences. The use of flame in the atomization minimizes interference effects. The most commonly used dissolution methods are based on acid attack and wet digestion.

Microwave digestion is a novel wet digestion technique for the dissolution and mineralization of the samples for elemental analysis. Due to the rapidity of heating, efficiency, and ease of automation, this technique is very convenient for the preparation of a diverse range and a large number of samples. Despite the advantages, there are a few drawbacks associated with the AAS measurements. It is available only at well-established laboratories, and qualified personnel are required to run the instruments. With these points in the study of the migration behavior of AcF considered, a cheap, simple, and reliable measurement technique, which is commonly used in almost every laboratory, was proposed.

Hence, the colorimetric measurement of AcF was selected to follow the migration behavior in the HTPB-based elastomeric structure. The performance of the method was evaluated by a comparison of the results with those obtained by AAS.

EXPERIMENTAL

Materials

HTPB (R-45M) was supplied by ARCO Chemical Co. (Philadelphia, PA) The average molecular weight of R-45M was 2975 g/mol, and the hydroxyl content was 0.65 mmol/g. The prepolymer was composed of approximately 20% *cis*-1,4 structure, 60% *trans*-1,4 structure, and 20% vinyl-1,2 structure. The curing agent [toluene diisocyanate (TDI)] was obtained from Fluka AG (Switzerland). Dioctyl adipate (DOA) and AcF (95%) were supplied from ACROS Organics (Belgium) and were used as received. Polyfunctional aziridine in a solution of ethylene glycol monoethyl ether (AST D45+) was provided from Kimetsan (Ankara, Turkey).

Apparatus

Atomic absorption spectrophotometric analysis (AAS), ultra-violet spectro-photometric (UV-VIS) analysis were made on air/C_2H_2 flame type Philips PU 9200 AAS spectrophotometer (England) at a wavelength of 243.8 nm and a Shimadzu UV-160 instrument (Kyoto, Japan) at a wavelength of 330.5 nm, respectively. For AAS analyses, leaching of acetylferrocene from samples is fulfilled by a closed-system acid dissolution procedure. A Milestone Ethos Plus 2 Shelton (CT) microwave dissolution system was used for the closed-system dissolution procedures. Maximum power of the system, controlled by a temperature sensor, was 1000 W.

Preparation of test specimens for the migration studies

The samples with barriers, used to investigate migration behavior, were prepared at three stages to simulate the original region of propellant in which the migration process took place. The three layers were called the nonadditive, barrier, and additive layers and corresponded to the insulation, liner, and propellant grain layers, respectively, in the original applications. All three layers were cured for 3 days before aging. The nonadditive part, which was only composed of HTPB–TDI, was prepared first. Next, the barrier layer with a composition of HTPB–TDI–AST D45+ (polyfunctional aziridine) was molded on the primarily prepared nonadditive part. Finally, the third layer, which it included both plasticizer (DOA) and ferrocene derivative (AcF), was molded and cured (for 3 days) on the surface of the barrier layer. In this study, samples with no barrier were also prepared to characterize the migration of the ferrocene derivative and also to compare whether the barrier layer used in some of the samples worked or not.

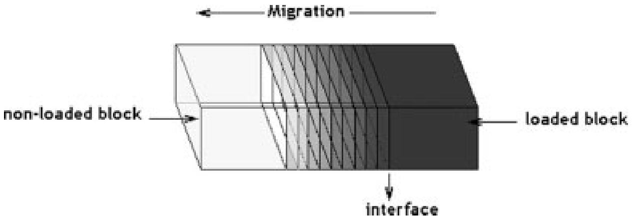

Figure 2 Slices of the elastomeric specimen.

Aging and spectral studies

Prepared samples were aged in air at 60°C for previously considered time intervals. The same aging program was applied to the specimens both with barriers and without barriers. After aging, slices obtained from the blade cutting of samples were chopped and weighed into desired amounts of sample for extraction. For the UV–vis technique, AcF was taken from slices with dichloromethane. For AAS analysis, the leaching of AcF from the samples was fulfilled by a closed-system acid dissolution procedure. AcF concentration was then calculated from the concentration of Fe(III) in the aqueous solution obtained from the acid dissolution procedure.

RESULTS AND DISCUSSION

Characterization of AcF migration by UV–vis spectroscopy and AAS

The migration of mobile components was studied by measurement of the ferrocene base burning-rate catalyst (AcF) concentration in the HTPB-based elastomeric system at various distances from the interface between the loaded and nonloaded blocks at definite intervals of aging. Consequently, the elastomeric systems were cut into slices, and the distance of each slice from the interface was settled, as shown in Figure 2.

Each slice was chopped into small pieces, mixed homogeneously, and divided into two equal portions for the determination of AcF concentration with AAS and the colorimetric technique.

For AAS measurement, suitable flame and spectrometric conditions were selected for iron determination. Dissolutions were conducted by microwave digestion, and parameters such as the microwave power

TABLE I
Swelling Values for Several Solvents

Solvent name	Swelling % (w/w) after 12 h
Benzene	429.4
Methanol	1.3
Diethylether	192.0
n-Hexane	103.5
Dichloromethane	528.2

TABLE II
Results of the Improved Extraction Method

	UV–vis (mg/g of slice)	AAS (mg/g of slice)
Old extraction method	5.72	5.98
New extraction method (+30 min vortex)	5.82	—
New + (30 min + 30 min vortex)	0.13	5.98
Total	5.95	5.98

applied, exposure time, and composition of the digesting acids were optimized.

Samples for calorimetric measurement were prepared by the extraction of AcF into an organic solvent. To take out the analyte effectively from the crosslinked polymeric network, we examined the swelling character of the polymer in various organic solvents. The results are given in Table I.

As shown in Table I, the HTPB elastomer swelled to 528.2% (w/w) in dichloromethane. Furthermore, dichloromethane did not have any absorption around 330.5 nm. Therefore, it was the most suitable solvent for the AcF release studies.

One of the prepared samples was analyzed by both AAS and UV–vis spectroscopy, and the results were processed. According to the obtained mass concentration profiles of AcF, the two methods had the same sensitivity at lower concentrations. Almost the same results were obtained, and the AAS data was slightly higher for the first three specimens. After a certain concentration level, AAS became more sensitive. In this region, the AAS measurements were higher than the UV–vis measurements. This behavior is illustrated in Figure 3. Figure 3 also exhibits the gradual change in the AcF concentration at various distances from the interface.

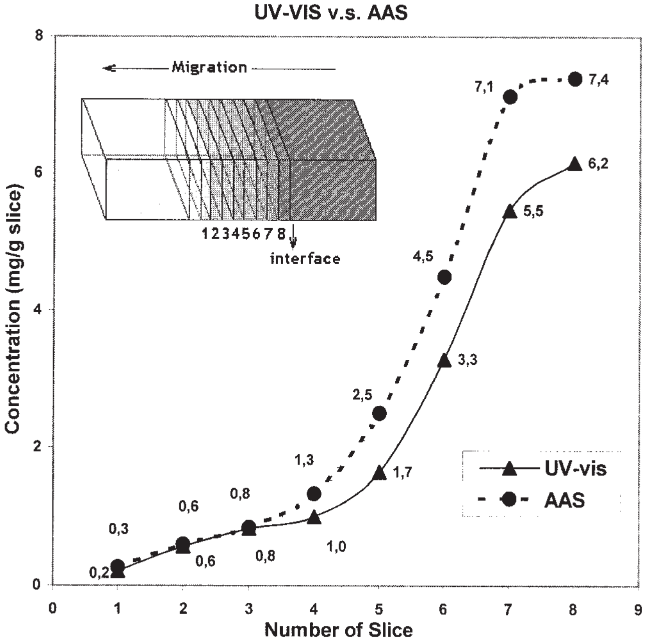

Figure 3 Mass concentration profiles of AcF evaluated by AAS and UV–vis methods after storage of the HTPB sample at 60°C for 3 days.

When slices taken away from the barrier were analyzed, the results obtained by colorimetric method were lower than those of the AAS method, and the difference was at a maximum for slice number 8 placed just after the barrier.

The amount of AcF to be extracted was the highest at this point; hence, the inefficiency of the extraction process could have been the reason for the low results.

Consequently, the extraction procedure was modified by the addition of an agitation step to increase the interaction of the polymer with the solvent. Instead of soaking the samples for 6 h in the solvent, we vortexed the samples.

In the previously used extraction method, chopped elastomer sample was swelled in dichloromethane solvent ($CHCl_2$), and extraction was done by two sets of washing for 3 h without any shaking; in each case, 5 mL of solvent was used. To increase efficiency, a second set was carried out with the help of a vortex shaker at 1500 rpm for 30 min. Even using vortex for only 30 min gave better results than 3 h without shaking. The further extraction runs were also applied to the same sample. Two additional 30-min extraction sets at 1000 rpm, each with 5 mL of solvent, were used. A significant amount of AcF was extracted with the additional sets, which meant that the extraction efficiency was increased by means of simple methods. The results are given in Table II.

The results obtained after this modification were almost the same for the both the AAS and UV–vis techniques. After all, it can easily be said that the UV–vis technique is still a more simple and practical method than AAS method, which requires a long acid dissolution procedure.

Therefore, we concluded that the proposed colorimetric method could be safely used to follow the migration behavior of AcF in a crosslinked elastomeric system.

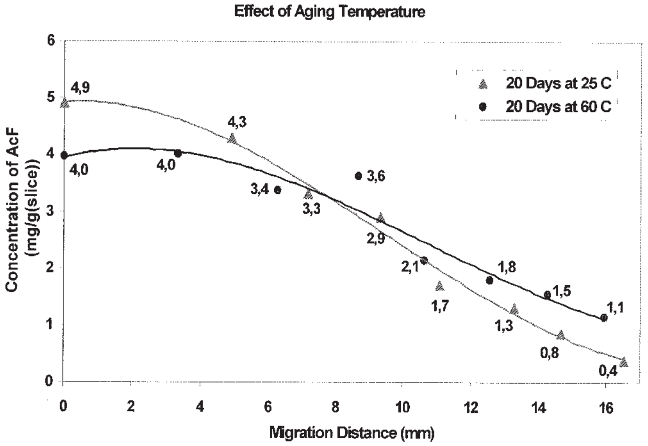

Figure 4 Effects of aging temperature on the migration of AcF in a HTPB-based matrix with no barrier.

Effect of aging temperature

The effect of aging temperature was studied and profiled for the samples aged for 20 days at 60°C. Figure 4 indicates that the temperature exhibited a strong influence on the AcF migration. In this part, one of two samples was aged for 20 days at 60°C; the other one was kept at room conditions for the same time interval. At first sight, there was a concentration gap between the two additive blocks at the migration distance interval between 0 and 6 mm of the specimens. This could be attributed to the higher evaporation of AcF from the surface of the specimen at a higher aging temperature. The accelerating effect of temperature on the migration rate for aged samples at 60°C could have been the reason the AcF concentration decreased from 1.5 to 0.8 mg/g of slice at about 14 mm of the migration distance. The same trend was observed beyond the interlayers of the samples (9–16 mm). It was obvious that the migration was dominated by the increasing temperature.

Effect of aging time

The aging time effect is very important because the plasticizer and burn-rate catalyst will continue to migrate for the entire lifetime of the rocket motor, reducing the concentration in the grain part. The time effect on migration was studied with specimens containing both 3% DOA and 0.9% AcF aged at 60°C in the range 1–15 days. In Figure 5, the total migration profiles are plotted for the specimens with no barrier. The results indicate the intensification of migration to a considerable extent with increasing aging time. These data indicate that the nonadditive region within 1–2 cm from the interface had a gradual change in the mass concentration of AcF. From these data, we inferred that there was a significant amount of AcF migration during the curing process. Therefore, the nonadditive region closer to the interface was significantly affected by migration even after this relatively short aging period. These results indicate that the AcF had migrated from the additive parts adjacent to interface into the nonadditive part. In Figure 5, the aging time of 0 days indicates the end of the curing process and the starting point for the aging process. Starting from 0 days, there was a regular increase in migration to the higher concentrations, and the further distances of the samples reached a maximum for the sample aged for 15 days.

Effect of barriers

The migration phenomenon occurs mainly due to the differential concentration of AcF between the additive part and the nonadditive part. Normally, it is assumed that when the concentration of AcF in these parts is equal, no migration can occur. It has been reported that the encapsulation of the propellant grain or somehow the immobilization of migrating species can sig-

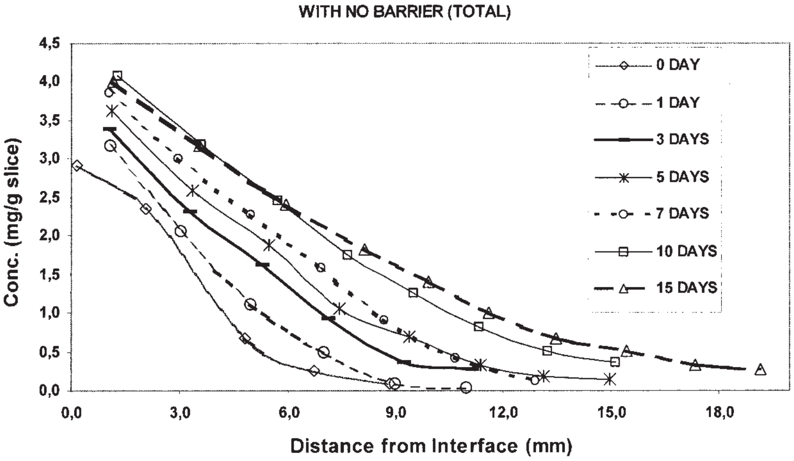

Figure 5 Overall migration profiles for the specimens with no barrier.

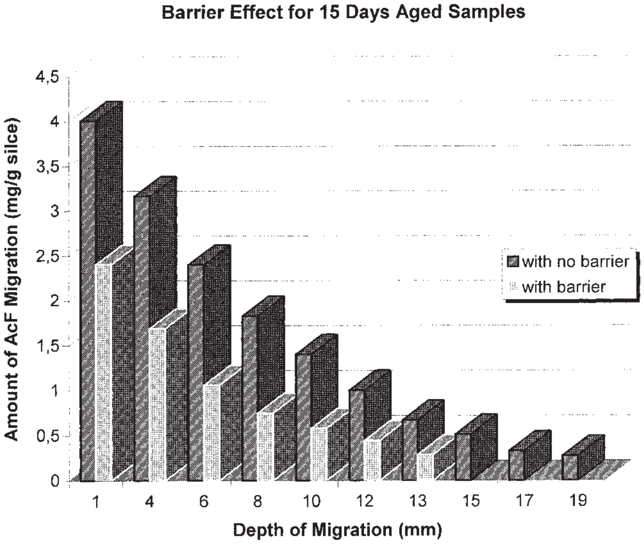

Figure 6 Effect of the barrier used for the minimization of AcF migration in samples aged for 15 days.

nificantly minimize a mobile additive's migration.[13] However, further study is necessary to minimize the migration. In this study, we used a highly crosslinked layer between the additive and nonadditive parts to minimize the migration. According to the data from Figure 6, there was a considerable difference in the amounts of migrated AcF at every distance. As a result, the barrier used in this system worked properly. Indeed, there was no AcF detected after 13 mm of migration distance.

Comparison of the total migration results

The total migration profiles for the samples with barriers are plotted in Figure 7. As evident from a comparison of the profiles in Figures 5 and 7, there were significant differences between the migration behaviors of samples without barriers and with barriers. In the case with no barriers, migration increased gradually with aging time because of there was no hindrance. The migration of AcF in these samples reached a maximum value somehow. This was deduced from the migration profile plots for samples aged 10 and 15 days in Figure 5. These plots are quite similar especially in first 10 mm migration distance. As previously discussed, migration was minimized in significant amount by means of the highly crosslinked layer. As a result of this, the migration process reached equilibrium earlier than the case in which samples without barriers were investigated. This behavior clear in Figure 7.

As shown in Figure 7, the migration level reached the top value at the end of 7th aging day. After that, a concentration decrease was observed due to evaporation of AcF from the surface of the samples. The evaporation from the surface and the migration process were competing with each other. The former could only overcome the latter because the latter would reach equilibrium. This relationship is supported also by Figure 7.

Determination of the diffusion coefficient

The behavior of migration for most low-molecular-weight fragments obeys, only in certain cases, Fick's law of diffusion.[14] Usually Fick's law applies to polymers possessing a flexible rather than a stiff backbone. Diffusion in an isotropic medium is given by eq. (1). If the amount of the migrant (AcF) at t is M_t and with the assumption of long migration times and a D value

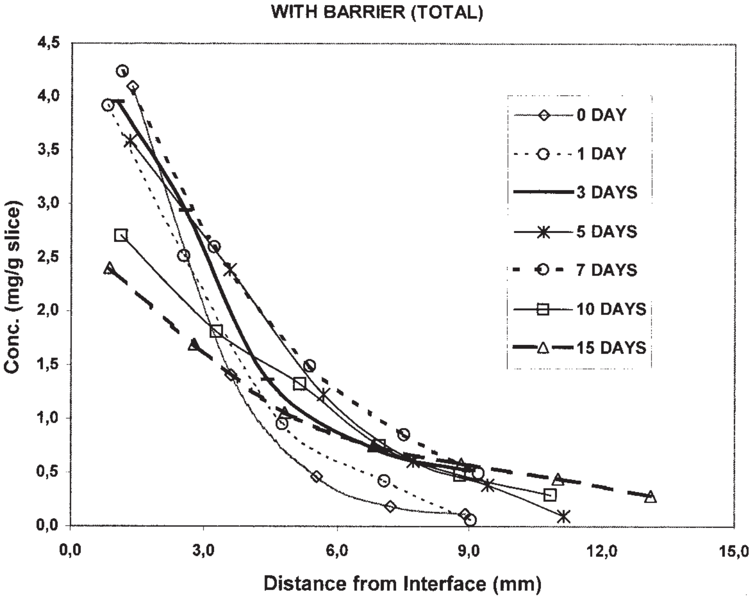

Figure 7 Overall migration profiles for specimens with barriers.

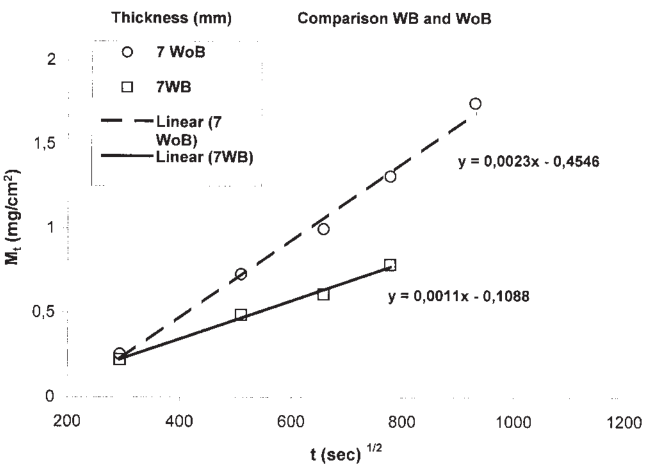

Figure 8 Plot of M_t versus the square root of t for AcF into HTPB-based elastomer samples with barriers (WB) and without barriers (WOB).

independent in concentration, eq. (1) can be reduced[14] to

$$M_t = 2C_{\mathrm{po}}(Dt/\pi)^{1/2} \tag{2}$$

Equation (2) can be used for the initial stages of migration, where M_t is expressed in mg/cm^2 and C_{po} is the initial concentration of AcF in the slice expressed in mg/cm^3.

In Figure 8, the plot of M_t against t is linear. From data given in Figure 8, the diffusion coefficients for both migrations in the samples with barriers and with no barriers were calculated by means of eq. (2). Both samples were aged for 7 days at 60°C. The same trends were also achieved for the samples aged for 3, 6, and 7 days and are given in Figures 9 and 10. For calculation, M_t is the amount of AcF migrated in t expressed in mg/cm^2 and C_{po} is the initial concentration of AcF in the sample expressed in mg/cm^3. D was found to be 2.69×10^{-10} cm^2/s for the sample without barrier and 6.15×10^{-11} cm^2/s for the sample with barrier, which was much lower than the former. From the calculated diffusion coefficient values, we can easily say that the migration of AcF in the HTPB-based elastomer was minimized significantly by increasing crosslink density in the interface layer between the loaded and nonloaded blocks.

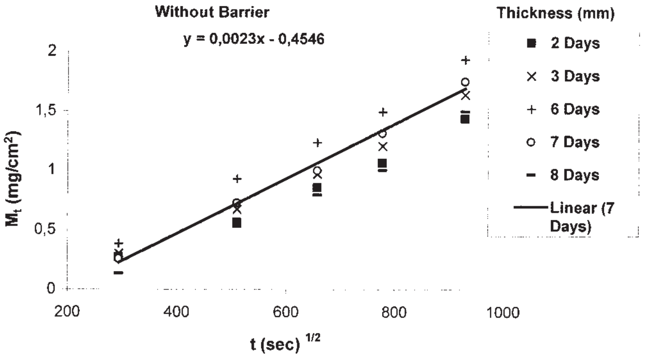

Figure 9 Plot of M_t versus the square root of t for AcF into HTPB-based elastomer samples without barriers aged for several days.

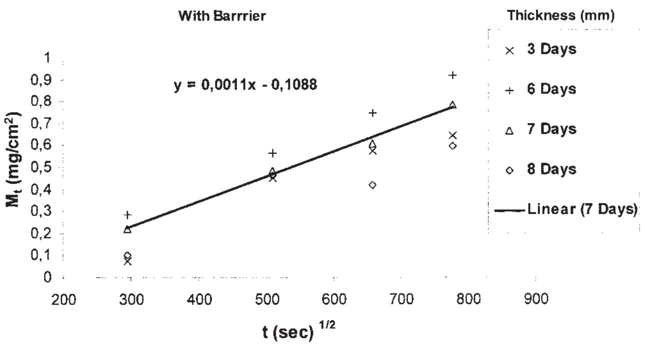

Figure 10 Plot of M_t versus the square root of t for AcF into HTPB-based elastomer samples with barriers aged for several days.

CONCLUSIONS

AcF migration was found to be time and temperature-dependent. Due to the hindrance effect of the highly crosslinked layer, vaporization from the surface of the sample became more important at the end of 7 days of aging at 60°C. After reaching equilibrium in the samples with barrier, AcF concentration decreased, especially at the higher concentration region. Also, as anticipated, the migration was augmented by increasing aging temperature.

In this study, diffusion coefficients were calculated to make deductions about the migration behaviors of AcF in samples both with barrier and with no barrier. The comparison of these two D values showed that the barrier layer, which was constituted between the loaded and nonloaded blocks, caused a significant reduction in the amount of the migration of AcF in the HTPB-based elastomer system.

A very practical colorimetric method was proposed to follow the change in AcF concentration in the system. This technique required virtually no sample preparation. Another technique, flame AAS, which is particularly suitable for metal analysis, was also used for data collection. The evaluation of the results gathered from these two techniques showed that colorimetric method could safely be used for the determination of AcF in solid propellant systems.

References

1. Keizers, H. L. J. In International Symposium on Energetic Materials Technology; American Defense Preparedness Association: 1995; p 200.

2. Lu, Y.-C.; Kuo, K. K. Thermochim Acta 1996, 275, 181.
3. Sell, T.; Vyazovkin, S.; Wight, C. A. Combust Flame 1999, 119, 174.
4. Torry, S.; Cunliffe, A. In Proceedings of the 31st International Annual Conference of ICT, Karlsruhe, Germany, Ziegahn, K. F., Ed.; Fraunhofer: Pfinztal, Germany, 2000; p 25.1.
5. Menke, K.; Gerber, P.; Geissler, E.; Bunte, G. Propellants Explosives Pyrotechnics 1999, 24, 126.
6. Christiansen, A. G.; Layton, L. H.; Carpenter, R. L. J Spacecraft 1981, 18, 211.
7. Swett, M. In AGARD PEP Symposium on Service Life of Solid Propellant Systems Athens, Greece, May 10–14, 1996; NATO Research and Technology Organization, Ed.; Canada Communication Group Inc., AGARD-CP-586, 1997; Section 4–1.
8. Venkatesan, D.; Srinivasan, M.; Reddy, K. A.; Pendse, V. V. Polym Int 1993, 32, 395.
9. Niehaus, M.; Kelzenberg, S.; Bunte, G. In Proceedings of the 31st International Annual Conference of ICT, Karlsruhe, Germany, Ziegahn, K. F., Ed.; Fraunhofer: Pfinztal, Germany, 2000; p 57.1.
10. Sutton, G. P. Rocket Propulsion Elements: An Introduction to the Engineering of Rockets, 6th ed.; Wiley: New York, 1992.
11. Davenes, A. Solid Rocket Propulsion Technology; Pergamon: Elmsford, NY, 1993.
12. Subramanian, K. J Polym Sci Part A: Polym Chem 1999, 37, 4090.
13. Swarts, P. J.; Immelman, M.; Lamprect, G. J.; Greyling, S. E.; Swarts, J. C. SAfr Tydskr Chem 1997, 50(4), 208.
14. Goulas, A. E.; Kontominas, M. G. Z Lebensm-Unters-Forsch 1996, 202, 250.